Available online at www.sciencedirect.com
ScienceDirect
Estuarine, Coastal and Shelf Science 70 (2006) 599–612
ESTUARINE COASTAL AND SHELF SCIENCE
www.elsevier.com/locate/ecss

Numerical investigation of the effects of upwelling on harmful algal blooms off the west Florida coast

Lyon W.J. Lanerolle [a,*], Michelle C. Tomlinson [b], Thomas F. Gross [a], Frank Aikman III [a], Richard P. Stumpf [b], Gary J. Kirkpatrick [c], Brad A. Pederson [c]

[a] *Coastal Survey Development Laboratory, NOAA, National Ocean Service, 1315 East-West Highway, Silver Spring, MD 20910, USA*
[b] *Center for Coastal Monitoring and Assessment, NOAA, National Ocean Service, 1305 East-West Highway, Silver Spring, MD 20910, USA*
[c] *Mote Marine Laboratory, 1600 Ken Thompson Parkway, Sarasota, FL 34236, USA*

Received 1 June 2006; accepted 1 June 2006
Available online 7 August 2006

Abstract

The initiation of the toxic harmful algal bloom (HAB), *Karenia brevis*, along the west Florida coast has been associated with upwelling events. Upwelling processes may be responsible for the transport of nutrients or algae from deep offshore locations across the Florida shelf to the coast. The influence of coastal wind-driven upwelling on the onset and occurrences of *K. brevis* in this region was numerically investigated using Rutgers University's Regional Ocean Modeling System. Computations were carried out in an idealized model domain, a two-dimensional slice in the cross-shore and vertical directions. The surface forcing data used was from several offshore meteorological buoys. The motion of the algae was simulated using Lagrangian particles and a passive tracer. The numerical simulations of three *K. brevis* events in 2000–2002 showed that the particles respond (with upwelling/downwelling) to the along-shore wind stresses as expected and some upwelling was present during the events. Comparison of the passive tracer fields with measured fluorescence data exposed the model's sensitivity to the particular surface forcing data employed and the relatively more significant role played by surface forcing over initial conditions. The present model set-up constitutes a useful predictive tool for conditions conducive to the onset of HABs. It is planned to be used in a real-time mode to aid the NOAA HAB monitoring and forecasting system.

Keywords: *Karenia brevis*; upwelling; numerical modeling; Regional Ocean Modeling System (ROMS); Lagrangian particle path tracking; passive tracer

1. Introduction

Blooms of the toxic dinoflagellate, *Karenia brevis*, are a recurrent problem along the west Florida shelf and occur nearly annually. Impacts of these blooms include marine mammal and fish kills, neurotoxic shellfish poisoning and respiratory irritation in humans. Due to the deleterious effects and human health risks associated with *K. brevis* blooms, the National Oceanic and Atmospheric Administration (NOAA) has developed a Harmful Algal Bloom Forecast System (HAB-FS) in the Gulf of Mexico which became operational in October 2004 (Stumpf et al., 2003). The current capabilities for predicting the onset of *K. brevis* blooms along the West Florida coast during the bloom season has an 80% success rate (Tomlinson et al., 2004). Additional methods are under investigation for the improvement of these forecasts, including the association of upwelling favorable winds with HAB events.

A correlation between the occurrence of *Karenia brevis* on the west coast of Florida and upwelling favorable winds has been shown by Stumpf et al. (1998) and is currently used to predict the initial appearance of the bloom at the coast (Stumpf et al., 2003). This association between blooms and upwelling favorable conditions is consistent with the development of *K. brevis* blooms at depth and subsequent transport

* Corresponding author.
E-mail address: lyon.lanerolle@noaa.gov (L.W.J. Lanerolle).

0272-7714/$ - see front matter © 2006 Elsevier Ltd. All rights reserved.
doi:10.1016/j.ecss.2006.06.015

to the shore by onshore bottom flow (Li and Weisberg, 1999). This paper will numerically examine the influence of upwelling on the onset and occurrence of *K. brevis* and in particular the dynamics that occur within the water column. Some preliminary cross-shelf transport modeling of *K. brevis* blooms on the west Florida shelf has been conducted by Walsh et al. (2003) and Ly et al. (2004).

For this study, the Rutgers University's Regional Ocean Modeling System (ROMS) was used to perform numerical simulations. The computations are carried out in a domain that is a two-dimensional slice, so that the vast majority of the grid points are placed in the cross-shore and vertical directions with a few grid points (together with periodic/cyclic boundary conditions) in the along-shore direction. The advantage of the two-dimensional geometry is that whilst being computationally cheaper than a full three-dimensional model, it also allows very fine grid spacings in the vertical and cross-shore directions whereby nearly grid-independent numerical solutions can be achieved. Further details regarding the model, set-up, boundary conditions, etc. are given in the following section. The simulated motion of algae (*Karenia brevis*) within the water column is achieved via Lagrangian particle path tracking. In order to simulate natural conditions, measured data is employed in the construction of the model bottom bathymetry, initial conditions and atmospheric forcing. This paper will show that even with this relatively simple, two-dimensional model set-up, the numerical simulations yield useful insights into the dynamics of *K. brevis* within the water column and the onset of these blooms. Furthermore, this model set-up will also constitute a useful numerical tool that can be run in real-time in order to enhance the NOAA HAB prediction capabilities.

2. Model, method and applications

The Rutgers University's Regional Ocean Modeling System (ROMS) (Shchepetkin and McWilliams, 2004; ROMS, 2005) is a finite difference model using a orthogonal curvilinear grid system with a terrain following vertical discretization. The model has been applied to many water bodies of all scales, ocean basin, coastal and estuarine (Haidvogel et al., 2000; MacCready and Geyer, 2001; Dinniman et al., 2003; Lutjeharms et al., 2003; Marchesiello et al., 2003; Peliz et al., 2003). In terms of the numerics, the model has high-resolution, upstream-biased advection schemes tracers (Shchepetkin and McWilliams, 1998) and an extremely accurate and robust baroclinic pressure gradient algorithm. The surface forcing in ROMS is done using a bulk flux formulation (Liu et al., 1979; Fairall et al., 1996a,b) where wind velocities, air temperature, air pressure, air relative humidity and solar shortwave radiation data are all combined simultaneously to generate model wind stresses and heat fluxes in a coupled manner. This model has the capacity to either calculate the longwave radiation internally (Berliand approximation; Berliand and Berliand, 1952) or for it to be prescribed via data. If however the surface wind stress and (net) heat flux data is available then these quantities can be used in place of those mentioned above. Cloud cover and precipitation can also be included in the computations. Along the bottom bathymetry, the forcing is carried out by prescribing the bottom stresses via a linear, quadratic or logarithmic law. In addition to the surface and bottom forcings, ROMS also incorporates tidal forcing (with seven constituents) and river forcing. The lateral open boundaries can be treated in a number of ways including the use of closed, clamped to data, periodic and radiation conditions with and without nudging to boundary data. In addition to the standard Mellor–Yamada 2.5 vertical eddy-viscosity closure, there is a family of General Length Scale (GLS) closures which consists of the following members: Mellor–Yamada, k-epsilon, k-tau and k-omega (Warner et al., 2005). The ROMS model has the capacity to perform Lagrangian particle tracking (of mass-less and point-like particles) which will be employed in this research.

The computational domain consisted of a thin quasi two-dimensional slice emanating from (near) Sarasota, Florida and approximately perpendicular to the coast (Fig. 1); in the cross-shore direction, it was 872 km in length and in the along-shore direction it was 4 km in width, and all depths below 500 m were set to 500 m itself. Most of the grid points were placed in the cross-shore and vertical directions and a few points were included in the along-shore direction. Typically 5–7 grid points were used in the along-shore direction and the numerical solutions were not sensitive to the number of points used. The vertical grid point distribution was according to a terrain-following σ-parameterization (Song and Haidvogel, 1994). This vertical grid also enabled finer vertical grid spacings to be placed in the surface and bottom boundary layers for a uniform σ-distribution and it is specified such that:

$$z(\sigma) = \eta[1 + \{h_C\sigma + F(\sigma)(h - h_C)\}/h] + h_C\sigma + F(\sigma)(h - h_C);\ F(\sigma) = -\left|\left[1 - (1+\sigma)^{2\theta_s}\right]^{\theta_b}\right|$$

where $z = z(\sigma)$ is the physical depth associated with each sigma layer/value, η is the sea (free) surface height, $h_C = \min[T_{\rm cline}, \min(h)]$ so that $T_{\rm cline}$ is a surface/bottom boundary layer width in which higher grid resolution is desired, h is the bottom topographic depth and σ is the dimensionless vertical (sigma) coordinate spanning the range $[-1, 0]$ such that $\sigma = -1$ coincides with the bottom bathymetry and $\sigma = 0$ coincides with the ocean surface. The numerical parameters θ_s and θ_b allow control of grid point distributions and clustering density.

The coastal boundary condition was a closed space, land condition. The offshore boundary condition was a radiation/far-field condition (Marchesiello et al., 2001) for all variables including barotropic velocities and sea surface height, whose validity was ensured by making the cross-shore domain length sufficiently long. To insure a two-dimensional simulation, boundaries in the along-shore direction, which are normal to the coast, were prescribed using periodic/cyclic conditions.

As this model will be run using meteorological data from weather stations or buoys, the surface forcings will be calculated via the ROMS bulk flux routines. Then the required inputs are

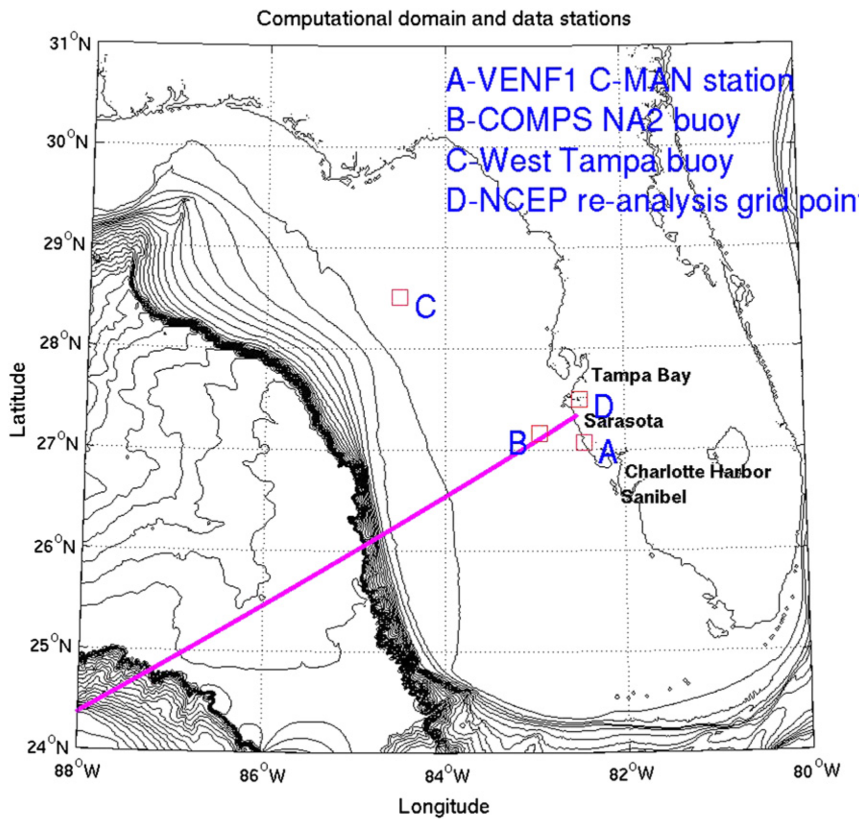

Fig. 1. Computational domain, bathymetry, buoys and data stations.

surface wind speed, air temperature, air pressure, air relative humidity data and measured or ROMS empirically/internally evaluated solar radiation (shortwave and longwave) data.

In terms of numerics, the third order upwind advection schemes for momentum and tracers are preferred in this study because they ensure that no explicit horizontal harmonic or biharmonic viscosity and/or diffusivity is necessary in order to generate numerically stable and smooth solutions.

The optimal model parameter set was discerned by performing idealized computations where the initial and surface forcing conditions were prescribed in a simplified sense. Thereafter, this set-up was also used in performing realistic simulations. The idealized calculations used to establish model parameters and the realistic simulations are described below.

2.1. Idealized case and calibration

For this idealized case, the initial conditions used were zero velocities (both baroclinic and barotropic), zero sea surface height, a constant salinity of 35 (PSU) and a linearly stratified vertical temperature profile, $T(z)$ where $T(0) = 25\ °C$ and $T(-500\ m) = 15\ °C$. For the ROMS bulk flux computations, the surface forcing conditions used which are constant in space and time are summarized in Table 1.

The shortwave radiation flux was prescribed empirically. These values are reflective of the summer conditions in Florida and the switching of the signs in the winds was to ensure that both upwelling and downwelling conditions could be simulated by ROMS. The initial model set-up was established using the Mellor–Yamada 2.5 closure (Mellor and Yamada, 1982) and the quadratic bottom stress formulations and thereafter, other choices for the turbulence closure schemes and bottom stress formulations were investigated. All of the model runs were for a duration of 180 days. This simplified system was used to test the effects of grid resolution, time step size, bottom stress formulation, vertical eddy-viscosity models, initial conditions and the importance of tides. The effects of each of these factors were determined by examining their influence on the flow-field (velocities and tracers) and also on the paths of some Lagrangian particles (mass-less and point-like) that were included in the computations.

2.1.1. Horizontal and vertical grid resolution and time step

In distributing points vertically, it is important to cluster them near the model ocean surface and also near the bottom in order to capture the surface and bottom forcings accurately; it was found that optimal clustering was achieved for the parameter set $\theta_s = 2.0, \theta_b = 7.0$ and $T_{\mathrm{cline}} = 50.0$. A horizontal grid resolution of 200–300 points was required to capture the essential spatial structure of the tracer fields. The cross-shore direction grid cell

Table 1
The atmospheric forcing data values for idealized ROMS set-up

Quantity	Value
Along-shore wind speed	±5 m/s
Air temperature	30 °C
Air pressure	1025 mb
Air relative humidity	70%

width in the near-shore region was 2000m. In the vertical, at least 60–80 levels were required to produce grid independent results. Time steps ranging from 100 s to 600 s were examined. The solutions were not found to be sensitive to this parameter. Hence, a grid consisting of 300 × 7 × 80 points and a time step of 600 s was found to be an acceptable choice.

2.1.2. Bottom stress formulation

The quadratic law with a drag coefficient of 0.003 was compared to the logarithmic law with a bottom roughness coefficient of 0.001. The spatial structure of tracers, velocities and particle paths was found to be quite similar and therefore the more commonly used quadratic law was retained for use.

2.1.3. Tides

Test cases were run with and without tides. The inclusion of tides did not significantly influence the temporal and spatial variation of the upwelling patterns or particle paths.

2.1.4. Vertical eddy-viscosity models

A comparison of the solutions from Mellor–Yamada 2.5 and General Length Scale (GLS) vertical eddy-viscosity closure models showed that the Mellor–Yamada 2.5 closure produced a distorted, unsmoothly varying and enlarged upwelling zone. The GLS models in general produced more clearly defined and smoothly varying upwelling zones. The numerical solutions and particle paths from the various GLS models were similar to each other. Some of these models depend on a surface roughness parameter and the examination of values in the range 0.004–0.1 m showed that the dependence was quite weak and hence negligible. In terms of the overall performance, clarity of upwelling/downwelling zones, particle paths, etc., the k-ω model was the best candidate and hence it was selected for use in this research from here onwards.

2.1.5. Initial conditions

The above-described simple initial conditions with a zero velocity field do not satisfy a geostrophic balance. As a consequence, they produce numerical solutions and volume-averaged kinetic energy time histories that suffer from initial inertial oscillations which sometimes lead to numerical instabilities. A better set of initial conditions were derived via a geostrophic balance which required two iterations; the first involved performing the geostrophic balance with a spatially constant density field and thereafter, feeding the resulting initial conditions into ROMS and producing a solution after a single time step which contained a density field corresponding to the satisfaction of a polynomial, non-linear equation of state in ROMS (Jackett and McDougall, 1995) and then repeating the geostrophic balance procedure with this latest density field. In both iterations, the numerical discretization of the pressure gradient terms was identical to that in ROMS. The barotropic velocities were obtained by vertically integrating the baroclinic velocities on the model grid. The sea surface height was set to zero. These new initial conditions were found to be in excellent geostrophic balance and the content of inertial oscillations present was negligible.

2.2. Realistic set-up

In the above idealized set-up, the bathymetry, although based on data, was quasi-analytical. In this realistic set-up, the bathymetry, initial conditions and surface forcing are all based on measured data to more closely simulate realistic scenarios. Each of these items is discussed below.

2.2.1. Bathymetry

The bathymetry along the model domain was formed by averaging the interpolated observed sounding data of five parallel transects—two to the north at 10 km apart and two to the south at 10 km apart of a central transect emanating from (near) Sarasota, Florida and approximately normal to the coastline. The bathymetric soundings data was from hydrographic survey data collected by NOAA (NOAA, 2004).

2.2.2. Initial conditions

The initial conditions were generated using T-S fields from the Modular Ocean Data Assimilation System (MODAS) data sets (Fox et al., 2001, 2002; MODAS, 2005) corresponding to the required initialization dates. The geostrophic balance procedure was performed to obtain the initial velocities.

2.2.3. Surface forcing

The surface forcing data sets consisting of air temperature, air pressure, air relative humidity, winds, shortwave radiation and longwave radiation fluxes were from several sources in the vicinity of the computational domain and where historical data was available (Table 2 and Fig. 1).

Before these data are employed in ROMS, they need to be quality controlled such that gaps are filled, extreme values are removed and missing data quantities are reconstituted by some means. The quantities that are most frequently missing are the relative humidity, the shortwave radiation flux and the longwave radiation flux. Relative humidity can be reconstituted if dew point data is available and shortwave and longwave radiation fluxes can be computed internally in ROMS via the Albedo formulation (Parkinson and Washington, 1979) and the Berliand (Berliand and Berliand, 1952) formulation. A sensitivity analysis study showed that the along-shore wind stress which is primarily responsible for upwelling/downwelling, is

Table 2
Sources of atmospheric forcing for the realistic ROMS HAB set-up

Name	Source	Device	Frequency
VENF1	Nat. Data Buoy Center (NDBC)/NOAA	C-MAN sta.	Hourly
COMPS NA2	University of South Florida	Buoy	20 min
WTAMPA	Nat. Data Buoy Center (NDBC)/NOAA	Buoy	Hourly
NCEP	Nat. Centers for Env. Pred. (NCEP)/NOAA	Numerical/ Re-analysis	6-hourly

not excessively sensitive to variations in the air relative humidity, solar shortwave and longwave radiation variables.

Hence, when there are substantial data gaps or even in the absence of any of these variables themselves, consistent numerical predictions can be achieved by substituting the missing data with reasonable empirical values.

Given in Fig. 2 is a comparison of the along-shore wind stresses resulting from the ROMS bulk flux formulation for the corresponding surface forcing data sets mentioned in Table 2. For September 2000, the VENF1 data could not be used due to significant data gaps and is therefore not plotted. The wind stress time series broadly follow each other with the closest resemblances seen between COMPS NA2 and NCEP in September 2000, between COMPS NA2 and VENF1 in 2001 and between COMPS NA2 and WTAMPA in early October of 2002. In September–October of 2002, the wind stresses show major disagreements between each other and the COMPS NA2 data even depicts a strong diurnal signal. As expected, the 6-hourly NCEP re-analysis data shows overly smooth variations with time and lacks detail. Despite these sometimes significant differences, during the HAB events (September 27, 2000; August 16, 2001; October 6, 2002—see the following section), at worst no downwelling is seen (NCEP re-analysis data) and at best upwelling favorable stresses are evident (VENF1, COMPS NA2 and WTAMPA data). Therefore, there is also some consistency between the different surface forcing data sets. The surface forcing data sets, VENF1 and COMPS NA2 were the favored choices due to their proximity to the computational domain. The former has the advantage that is a quality controlled, public domain product from NDBC/NOAA.

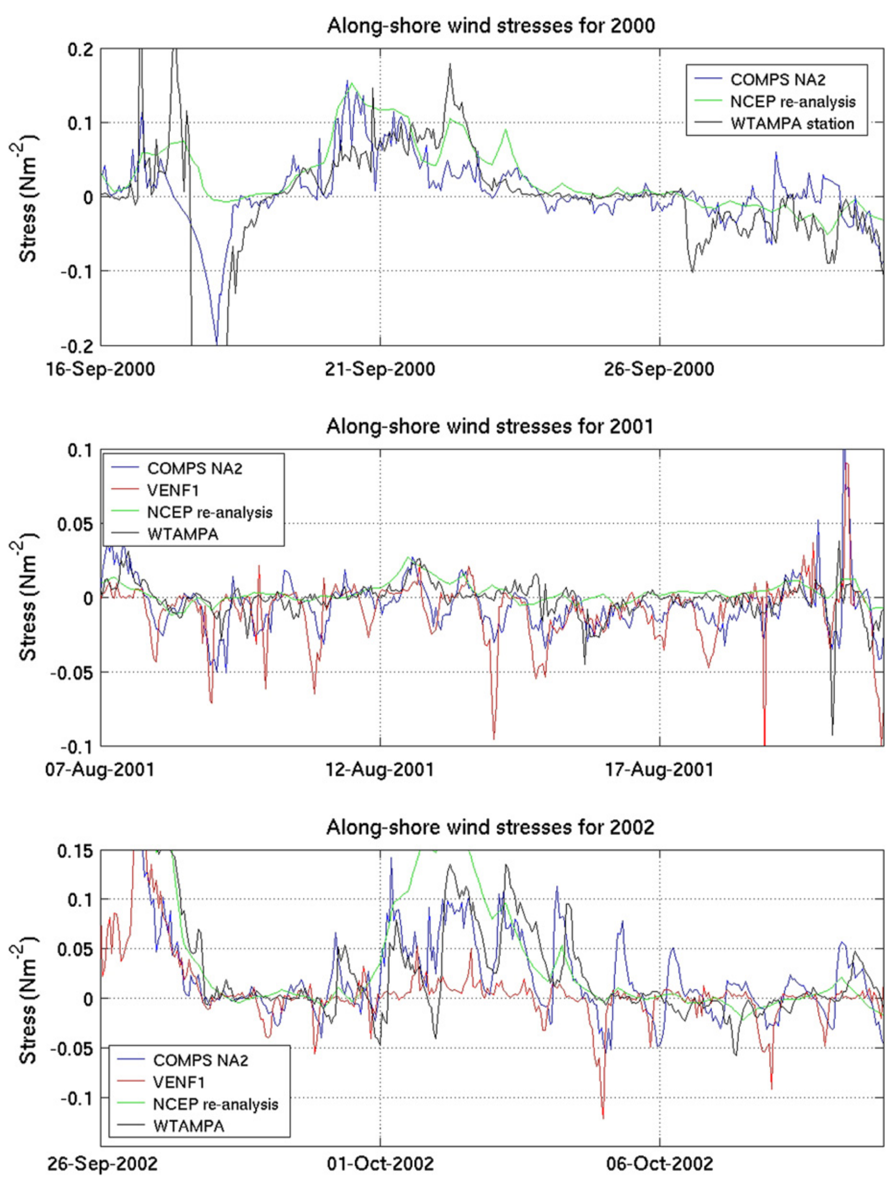

Fig. 2. Comparison of the ROMS generated along-shore wind stresses for 2000, 2001 and 2002 resulting from the VENF1, COMPS NA2, WTAMPA and NCEP re-analysis data sets.

2.3. HAB simulation strategy

Three HAB events were chosen to compare model simulations with known *Karenia brevis* blooms along the west Florida coast (Fig. 1). The first example represents a *K. brevis* bloom which developed in the Tampa Bay and Sarasota areas on September 27, 2000 (Stumpf et al., 2003). The second example began on August 16, 2001, where blooms were identified by satellite and field measurement off Sanibel Island through August 30. Relative fluorescence measurements along a vertical transect from August 14—September 27 of 2001 were carried out by an Ecology and Oceanography of Harmful Algal Blooms (ECOHAB) cruise and were used to compare the spatial density and transport of *K. brevis* to the coast. On September 3 of 2001, reports of respiratory distress and fish kills were reported in the Sarasota region. Northward transport of the bloom was identified by imagery and verified by field sampling (Stumpf et al., 2003). Following this event, the passage of tropical storm Gabrielle on September 14 expanded the *K. brevis* bloom. The third scenario represents a bloom offshore from Charlotte Harbor to Sanibel Island which was observed on October 6, 2002 following the passage of Tropical Storm Isadore.

The model runs were for a duration of 3 weeks beginning 2 weeks prior to an event and then continuing for a week after it. This ensured that besides an event itself, its onset could also be studied. If the model does predict an event too late, then that information too will be contained in the additional allocated time of 1 week.

The movement of the algae and in particular their response to upwelling and downwelling were simulated using Lagrangian particles which were mass-less and point-like although *Karenia brevis* are known to exhibit swimming behavior—see for example Gray et al. (2003), Steidinger and Joyce (1973). The particle tracks are expected to show the vertical as well as the cross-shore (onshore/offshore) motion of the algae. If the Lagrangian particles are introduced in a single ensemble at the start of the simulations then, in the 3-week duration, they are seen to disperse widely and their reaction to any particular upwelling/downwelling situation is difficult to discern. To improve visual clarity, multiple particle ensembles/populations were introduced at regular time intervals with identical

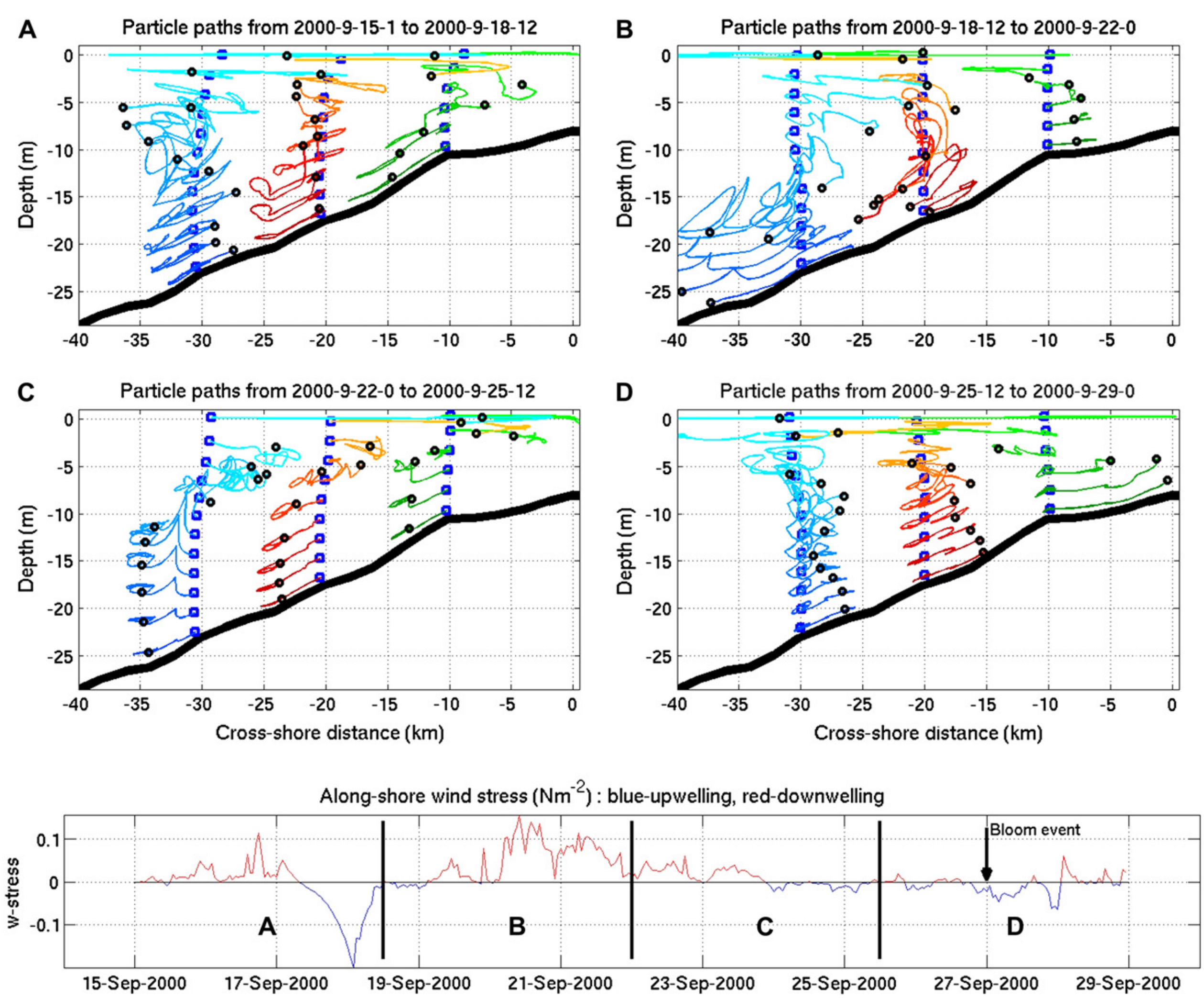

Fig. 3. The HAB event of September 2000. Particle paths and along-shore wind stress.

initial locations. Particles were introduced at 10 km, 20 km and 30 km distances from the coast and at several depths within the water column. The deepest particle was 1 m above the bottom and subsequent particles were spaced 2 m apart in the vertical. Four separate ensembles were introduced 3.5 days apart. This was done to ensure that the HAB events occurred 1.5 days after the introduction of the final ensemble, whereby the dynamics immediately preceding and immediately following the events would be apparent. The simulation of the ECOHAB relative fluorescence concentration experiment was done using a passive tracer in ROMS.

3. Results and discussion

The results pertaining to the three HAB events of 2000, 2001 and 2002 and the relative fluorescence experiment are discussed below.

3.1. HAB events of 2000–2002

The simulated particle paths corresponding to the movements of *Karenia brevis* for the three HAB events of 2000, 2001 and 2002 are depicted in Figs. 3–5. In these figures, the four panels represent the particle paths of the four different particle ensembles for a duration of 3.5 days each. The blue squares represent the initial particle locations and the black circles their positions after 3.5 days. The particle paths corresponding to an initial location of 10 km offshore are green in color, those at 20 km red in color and those at 30 km blue in color. Particle paths are shaded according to their initial depth with the color shades becoming progressively darker with increasing depth. Given also in each of these figures is a plot of the along-shore wind stress. Under the present model configuration, a positive stress (red) implies downwelling and a negative stress (blue) represents upwelling. The lettering associated with the four particle path panels (A, B, C, D) correspond to the annotated wind stress plot segments to facilitate a clear way to discern upwelling/downwelling behavior in the particle paths.

The September 2000 HAB simulation (Fig. 3) was carried out using only COMPS NA2 buoy data because the VENF1 data set had a significant data gap of 18 days. Initially, the wind stress is positive and remains so for about 2 days during which downwelling is induced and particles begin to move

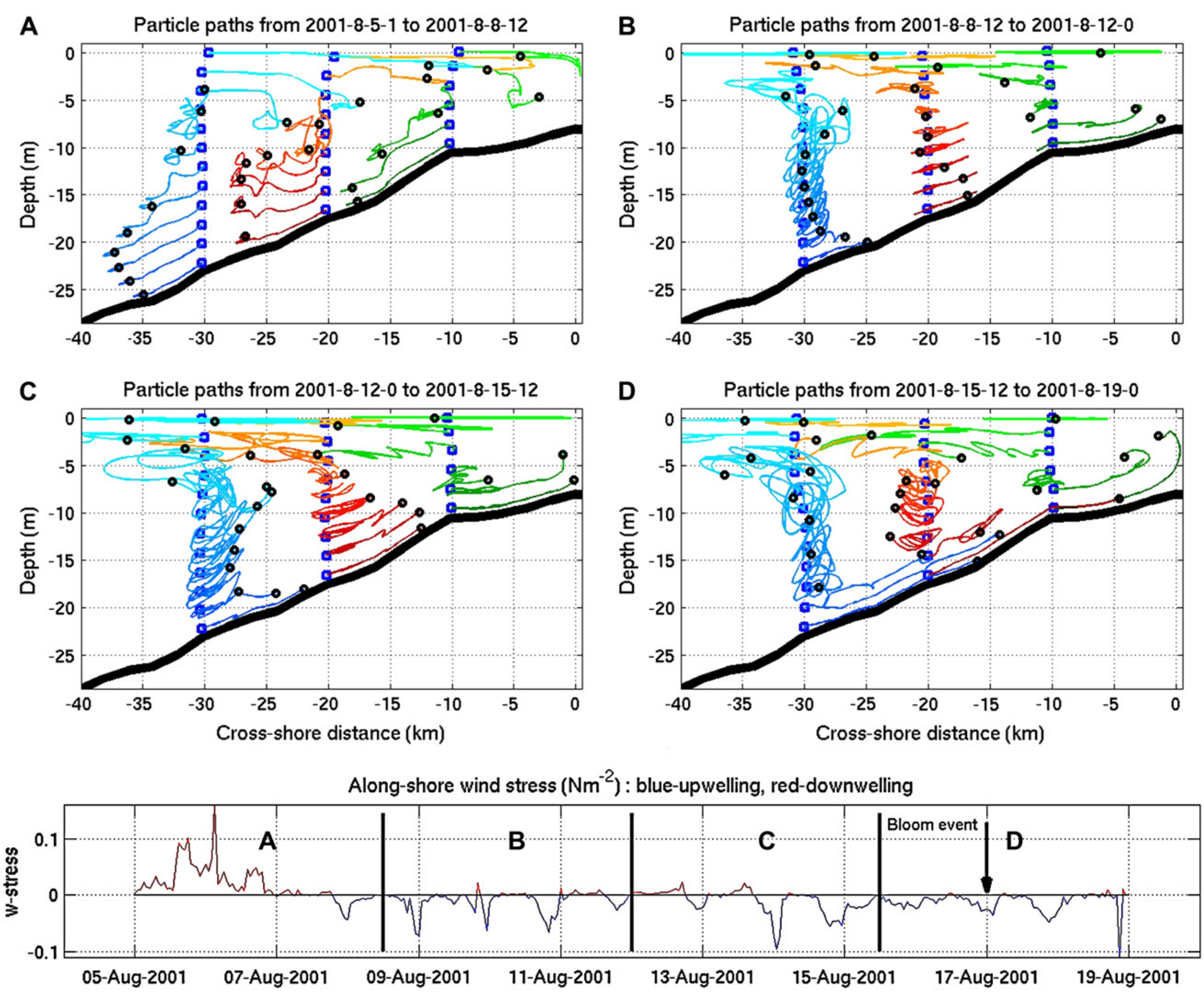

Fig. 4. The HAB event of August 2001. Particle paths and along-shore wind stress.

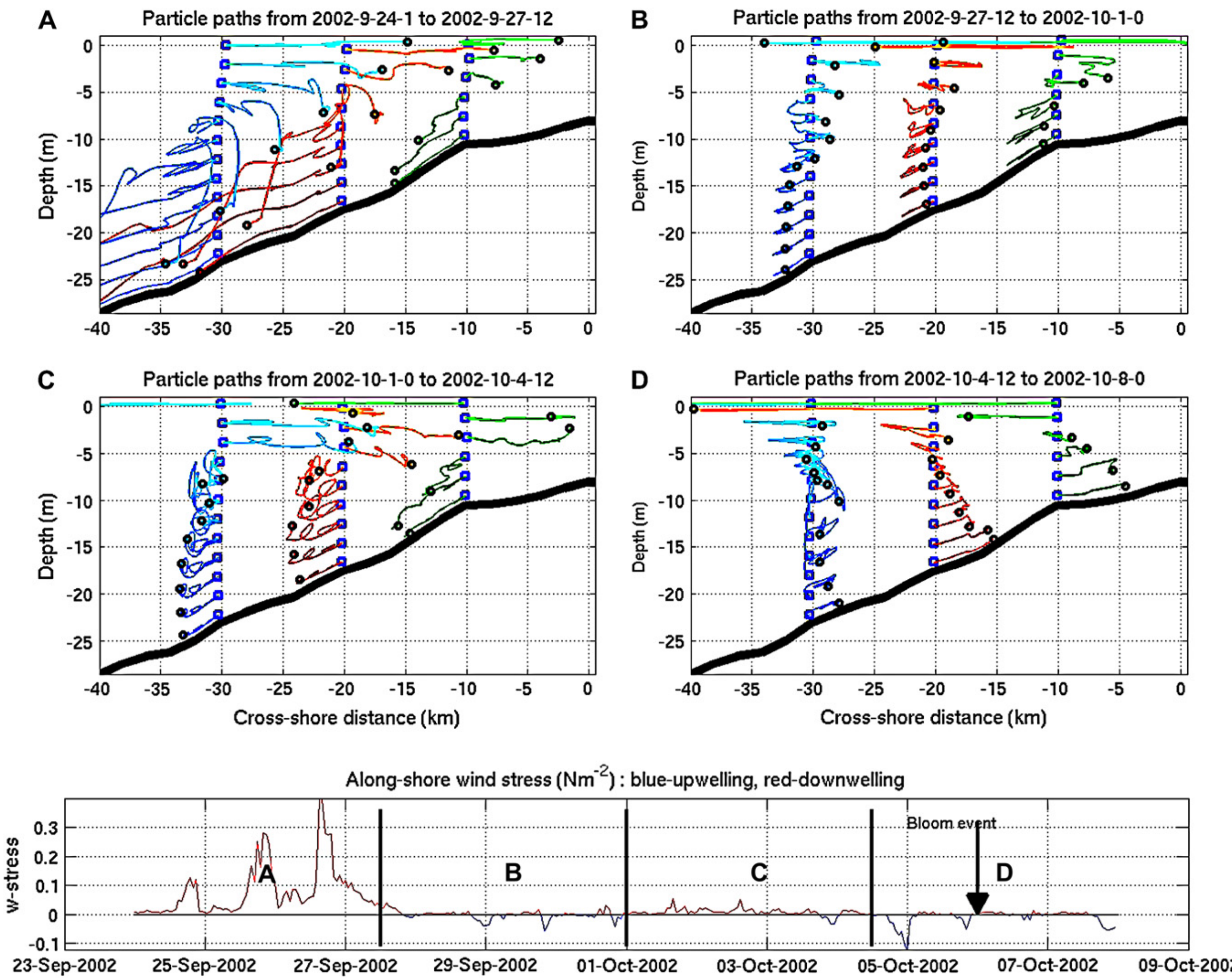

Fig. 5. The HAB event of October 2002. Particle paths and along-shore wind stress.

offshore and those close to the bottom also move down the water column, parallel to the bottom (panel A). Thereafter, an upwelling wind event lasting about half a day occurs around September 18 where the wind stress becomes sharply negative causing the near-bottom particles to reverse and move onshore and up the water column again, parallel to the bottom (panel A). The clearest response to the upwelling/downwelling is seen in the near-bottom particles. Panels B and C during which the wind stresses are mostly positive, mainly show downwelling and particles movement offshore. Around September 24, a weak upwelling develops (near the end of panel C) and persists until about September 28 during which particles are seen to move onshore and up the water column. The effects of a persistent weak upwelling wind stress are comparable to those of a strong event that lasts for a much shorter duration. In the vicinity of the bloom (September 27) an upwelling wind stress is present and particles move in the onshore direction and do so at an average rate of about 5–10 km in 3.5 days. Particles at the deeper depths show the clearest response to upwelling/downwelling wind stresses and move parallel to the bathymetry. The less predictable motion of the particles at intermediate depths is due to a transition in the vertical of the cross-shore velocity from an onshore configuration to offshore configuration or visa versa.

For the August 2001 HAB simulation (Fig. 4) the VENF1 wind data set was employed in the ROMS model runs. The computations begin with a strong downwelling wind stress, which causes particles to move offshore and into deeper waters (panel A). Beginning on August 7, a relatively long period of intermittent and weak upwelling is present leading up to and through the time of the bloom (panels B–D). This persistent upwelling causes the deepest particles in panels B, C and D to travel significant distances (for example, up to 20 km) onshore. Again, the particles in the mid-depths do not show a clear response to upwelling/downwelling wind stresses and an upwelling wind stress is present in the vicinity of the bloom. However, during the weeks preceding the August 17 bloom, upwelling occurred without the presence of a bloom.

The 2002 HAB simulation in Fig. 5 was also carried out using the VENF1 wind data set. As before, at the beginning of the computation a strong downwelling wind stress is evident (panel A) and thereafter both very weak upwelling and downwelling wind stresses are present (panels B–D). Hence, the onshore/offshore distances traveled by particles in this simulation after September 29 are much less than those in the 2000 and 2001 simulations. As before, near the time of the bloom (October 6), upwelling wind stresses are present and it is the deepest particles that show the clearest responses to the wind stresses and again, the upwelling at precisely the time of the event is not unique.

These model HAB simulations can be summarized as follows: (i) the particles respond to the upwelling and downwelling wind stresses faithfully and as expected, even the effects of weak upwelling/downwelling are apparent in the particle paths, (ii) the particle response to wind stresses is almost immediate, (iii) even weak wind-driven upwelling stresses are present preceding the HAB events, (iv) even weak upwelling wind stresses over a persistent period generate significant upwelling effects, (v) well prior to HAB events (7–10 days), strong downwelling wind stresses were seen, and (vi) the present model running format and graphical output format (Figs. 3–5) together provide a clear and useful numerical tool to predict upwelling assuming the onset of HABs are associated with the cross-shore transport of algae or nutrients; this is expected to contribute towards the development of a real-time, numerical, HAB prediction and analysis system.

3.2. Relative fluorescence experiment

Relative fluorescence measurements provided by an ECOHAB cruise during the 2001 event were used to indicate the concentration and location of *Karenia brevis* in the water column (Fig. 6). The red lines in the upper set of plots indicates the transect along which the fluorescence measurements were taken.

This scenario was emulated using ROMS by tracking the development of a passive tracer patch. The initial distribution of the tracer patch corresponded to the ‘‘blob’’ observed approximately 10 miles offshore from the 10 m isobath and at 15 m depth on August 14 and it was constructed with the use of algebraic functions. Initial conditions for the flow variables in the model simulations were provided by the MODAS data set as in the earlier HAB event simulations.

This simulation required the use of a finer grid in the cross-shore direction in the near-shore vicinity, with the grid spacing approximately 400 m, in order to capture the spatial structure of the passive tracer field in sufficient detail. The surface forcings were from the VENF1, WTAMPA and NCEP re-analysis data sets. This study also served to examine the differences and similarities in the simulations resulting from the use of the three different forcing data sets. The along-shore wind stresses from the three data sets are plotted in Fig. 7. It should be mentioned that around September 15, 2001 tropical storm Gabrielle passed over the west Florida coast region and its effects are included in the forcing data sets.

The model simulations and the ECOHAB cruise measurements (interpolated on to the ROMS computational grid) are shown in Fig. 8 for the four dates (August 14, August 27, September 10, September 26) when measurements were taken. The effects of the four different atmospheric data sources on the upwelling simulations are demonstrated. During the numerical simulation, the concentrations of the tracer patches diminish with time as expected due to diffusion and possibly along-shore transport. For each of the above dates, all three model results have been plotted using the same color scale

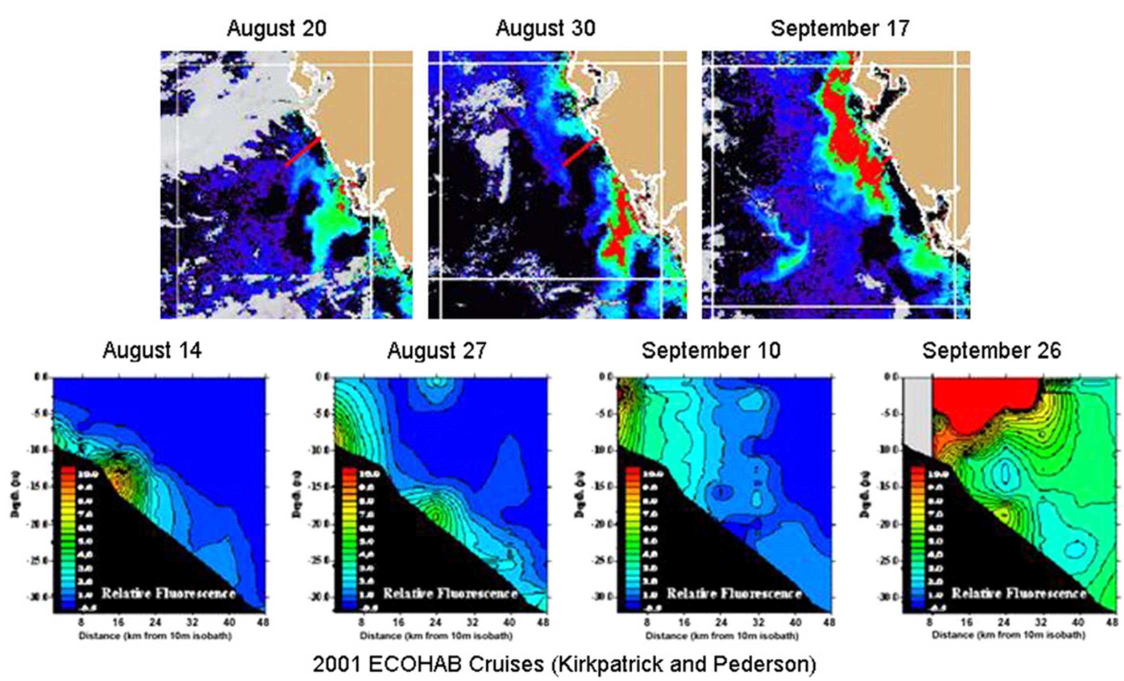

Fig. 6. Satellite imagery showing chlorophyll anomaly (upper row, after Stumpf et al., 2003 and Tomlinson et al., 2004) and relative fluorescence concentration measurements from the 2001 ECOHAB cruise (lower row, G.J. Kirkpatrick and B.A. Pederson). Red in the satellite indicates an anomaly of $>1\ \mu g\ L^{-1}$, which indicates a *Karenia brevis* bloom in these images.

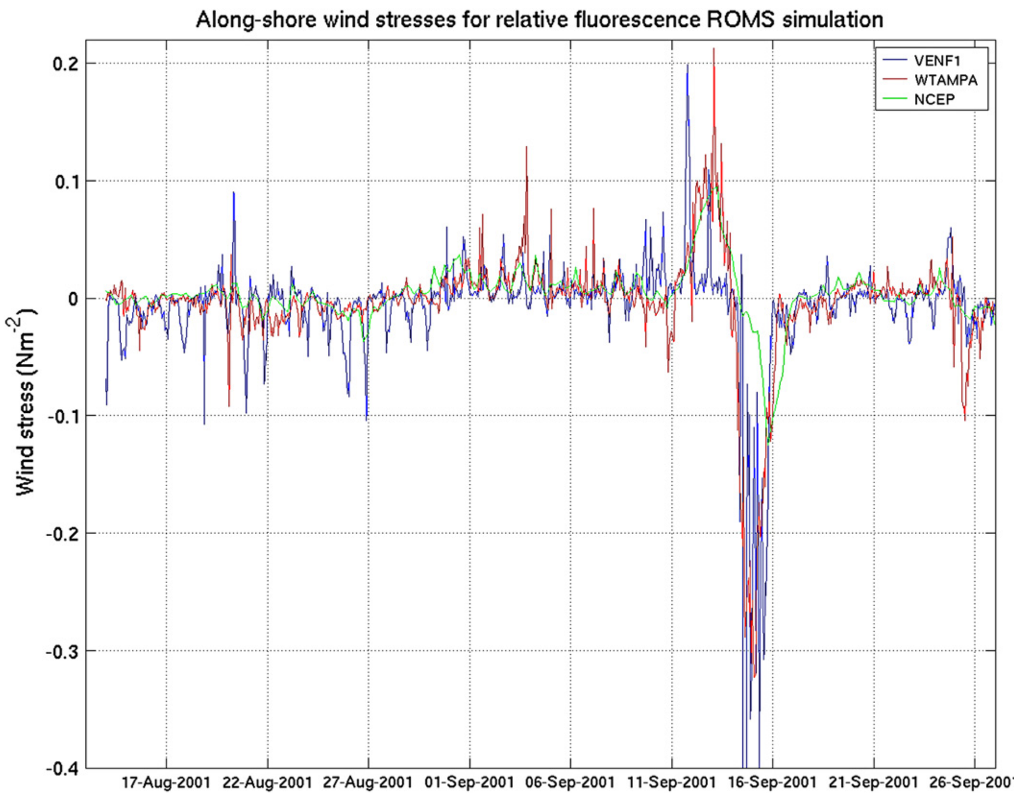

Fig. 7. A comparison of the ROMS generated along-shore wind stresses using the VENF1, COMPS NA2 and WTAMPA data sets for the relative fluorescence experiment (August–September 2001).

so as to make them directly intercomparable. The first vertical column in Fig. 8 shows the initial conditions (for August 14).

The model results for August 27 indicate that those due to the VENF1 and the WTAMPA data show excessive upwelling where the tracer patch has moved too far up the water column and that due to NCEP data is lagging behind/not upwelled enough relative to the measured data. These observations are consistent with the wind stress profiles of Fig. 7 where the greatest upwelling favorable wind stresses are seen to occur in the VENF1 data and the least for the NCEP data during the period August 15–25.

On September 10, the VENF1 tracer patch is diffused in space, perhaps due to the +/− variation in its wind stress and is downwelled through the water column due to favorable wind stresses near this date. The NCEP patch has been downwelled due to the purely positive, downwelling wind stress during the period September 1–10. The tracer patch due to the WTAMPA data shows the closest agreement with measurements and a downwelling wind stress is present around September 10; a second patch of tracer separates from the single tracer patch around September 3–4 and this is perhaps due to the spike in the wind stress also around this date with a possible contribution from the "bump" in the bathymetry which occurs around 10 km offshore.

The final panel of plots for September 26 shows some similarity between the results from the three forcing data sets although the VENF1 and NCEP results show a smeared tracer patch where the tracer concentration has been diluted. The similarity could be due to the strong effects of the storm around September 14–16 the presence of which is seen in all three of the forcing data sets. In the plot for the WTAMPA results, the two patches appear to have coalesced perhaps also due to the effects of the storm. The WTAMPA solution has the closest agreement with the measured data although the simulated tracer patch has not moved offshore as much as the observed patch. Around September 26, all three wind stress profiles in Fig. 7 indicate upwelling favorable wind stresses which appear to reform the vertical structure and move surface water offshore.

The ROMS numerical simulations were repeated using a different set of initial temperature and salinity conditions, with all other factors being identical. These initial conditions were formed by using the measured temperature, salinity and density anomaly data from the ECOHAB cruise for the first 50 km offshore and thereafter melding it with the MODAS data set for distances greater than 50 km. The melding was done in an elementary fashion using interpolation techniques within the framework of Matlab. The initial velocity field was calculated as before using the geostrophic balance approach. The numerical results and the measured data are given in Fig. 9, which can be contrasted to Fig. 8 that used only the MODAS based initial temperature–salinity fields. The plots show that while there are observable differences in

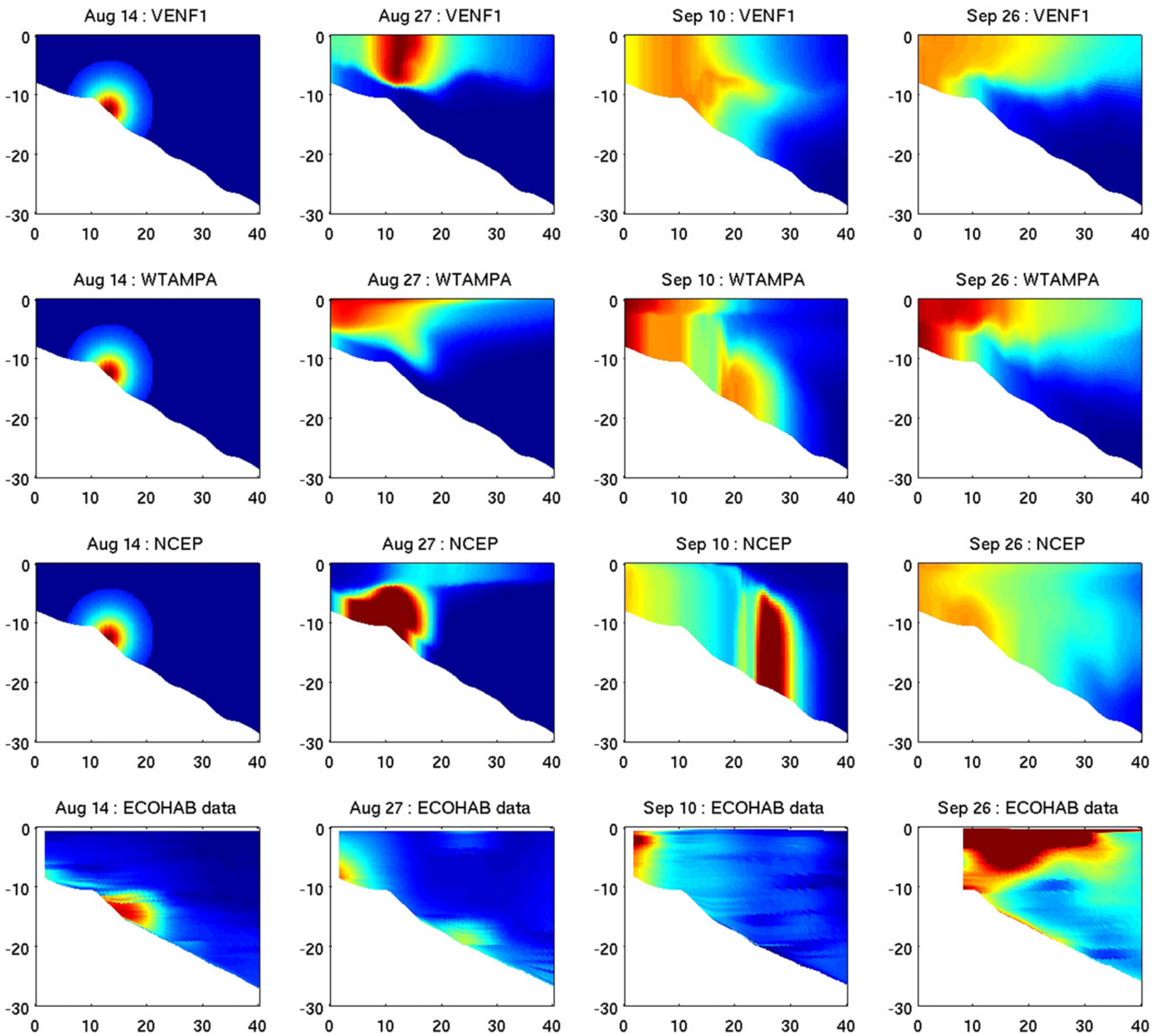

Fig. 8. Relative fluorescence model simulations (using the VENF1, WTAMPA and NCEP re-analysis data sets) and ECOHAB measurements (interpolated on to the ROMS grid). Initial conditions are from MODAS data. The color scale is as in Fig. 6.

the tracer patch structure and concentrations, the effects of using these initial conditions are not drastic and many of the inferences reached above are still valid. Hence, the differences in the development of the patches are much greater for the different surface forcing data sources than for the initial temperature–salinity fields.

4. Summary and conclusions

The ROMS model with surface forcing data from several observation sources and initial conditions from MODAS and ECOHAB cruise data were used to simulate HAB events and their onset by using Lagrangian particles and a passive tracer. The computational domain was a simplified two-dimensional geometry using cyclic/periodic boundary conditions in the along-shore direction. Even though this set-up did not contain the full three-dimensional effects, it had the advantage of being computationally cheaper and it allowed high grid resolutions in the vertical and cross-shore directions which would not be feasible in a three-dimensional computation.

An idealized computational set-up with uniform initial conditions and surface forcings enabled an optimal model parameter set (time step magnitude, number of horizontal and vertical grid points, σ-grid point distribution parameterization, bottom stress parameterization, eddy-viscosity model, etc.) to be determined which produced a numerically stable, robust and reliable model set-up. It was subsequently shown that the along-shore wind stresses, resulting from the ROMS model bulk flux formulation, were not sensitive to the prescription methods of the relative humidity, shortwave and longwave radiation which further enhanced the confidence associated with the model predictions.

The transition to realistic simulations involved the generation of a better bottom bathymetry from observed sounding

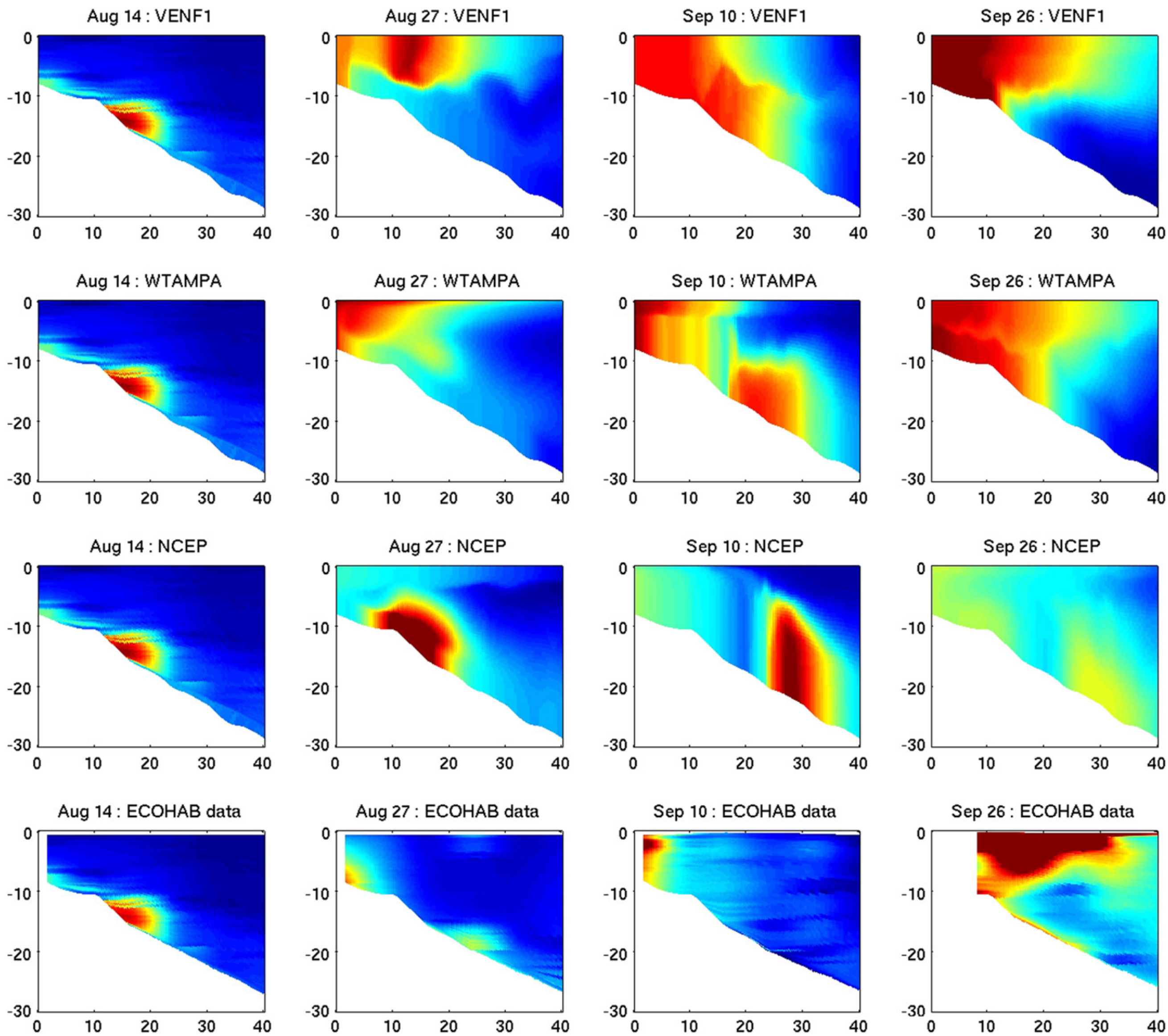

Fig. 9. Relative fluorescence model simulations (using the VENF1, WTAMPA and NCEP re-analysis data sets) and ECOHAB measurements (interpolated on to the ROMS grid). Initial conditions are from a melding of ECOHAB and MODAS data sets. The color scale is as in Fig. 6.

data, the use of real surface forcing data from buoys, C-MAN stations and the NCEP re-analysis procedure and the use of initial conditions for the temperature and salinity fields from the MODAS and ECOHAB data sets.

The 2000–2002 HAB event simulations and the ECOHAB relative fluorescence concentration simulations allowed the following conclusions to be reached:

1. The calibration and validation exercise carried out with the idealized computational set-up lead to a stable and reliable set-up which allowed real data-based bathymetry, initial conditions and surface forcings to be employed leading to the investigation of actual HAB events.
2. Even this simplified two-dimensional model set-up together with Lagrangian particle tracking and a passive tracer revealed useful insights into the motion of the algae (*Karenia brevis*) and the onset of HABs and in particular their response to wind-driven upwelling and downwelling situations. The behavior of the particles was consistent with the along-shore wind stress—that is, particles showed upward and shoreward motion in the water column when there was upwelling favorable wind stresses and visa versa.
3. The simulated HAB scenarios were seen to be quite sensitive to the surface forcing data set being used. As the surface forcing datasets often disagree with each other, the availability of reliable surface forcing data sets a crucial requirement. In the time period leading up to the HAB events, upwelling wind stresses were often encountered. Particle paths were seen to be sensitive to even small

upwelling/downwelling wind stresses and their response was immediate and without time lags. Long periods of weak upwelling result in effects that are comparable with strong upwelling wind events, which are of short duration.

4. Prior to each HAB event, the along-shore wind stresses indicated a period of downwelling, followed thereafter by upwelling. Although it has been observed that upwelling favorable conditions are responsible for the concentration and transport of offshore *Karenia brevis* cells at/to the coast, the effect of the downwelling prior to these events has not been described before. Perhaps these downwelling events serve as a preconditioning mechanism and may be necessary to initiate *K. brevis* blooms offshore, by providing conditions conducive to bloom development. It is possible, that the transport of necessary nutrients present in the coastal waters is being supplied by downwelling conditions.
5. The relative fluorescence concentration simulations showed that the model predictions are very sensitive to the surface forcing data set used as in the HAB event simulations above, and no particular wind dataset was obviously better than the others. However, the WTAMPA data did give reasonable results. As expected, major events like tropical storms and hurricanes are seen to have a significant impact on the dynamics of algae within the water column of these shallow waters. Although the use of different initial conditions did give observable differences in the numerical solutions of the near-shore regions, they were not drastic and the defining criterion is the surface forcing.

The research described in this paper has led to the development of a simple but useful tool to aid in the prediction of the onset of HABs and also to examine their dynamics due to upwelling. This model set-up will therefore be run in a real-time mode (for example, daily) after obtaining the necessary observed and model data inputs automatically from various sources including the Internet. It is planned to provide the results from this model to the NOAA HAB prediction system to give further guidance on upwelling conditions which may be useful to the HAB forecasters. Possible future enhancements include the addition of behavior (for example, swimming, buoyancy, etc.) to the Lagrangian particles and the passive tracer patches in order to simulate living organisms such as *Karenia brevis* better and extending this proven two-dimensional set up to three-dimensions.

Acknowledgments

We wish to thank Craig Lewis and Thomas Powell of UC Berkeley for providing the initial model set-up. We are also grateful to Mr. Vembu Subramanian of the University of South Florida for providing us with the COMPS NA2 buoy data. Partial support for this work was provided through the NOAA/National Ocean Service (NOS) Center for Sponsored Coastal Ocean Research MERHAB 2002 Program and through a NOS Partnership Project.

References

Berliand, M.E., Berliand, T.G., 1952. Determining the net longwave radiation of the earth with consideration of the effects of cloudiness (in Russian). Izv. Akad. Nauk SSSR, Ser. Geofiz 1.

Dinniman, M.S., Klinck, J.M., Smith, W.O., 2003. Cross shelf exchange in a model of the Ross Sea circulation and biogeochemistry. Deep-Sea Research Part II: Tropical Studies in Oceanography 50, 3103–3120.

Gray, M., Wawrik, B., Paul, J., Casper, E., 2003. Molecular detection and quantitation of the red tide dinoflagellate *Karenia brevis* in the marine environment. Applied and Environmental Microbiology 69 (9), 5726–5730.

Fairall, C.W., Bradley, E.F., Rogers, D.P., Edson, J.B., Young, G.S., 1996a. Bulk parameterization of air-sea fluxes for tropical ocean-global atmosphere Coupled-Ocean Atmosphere Response Experiment. Journal of Geophysical Research 101, 3747–3764.

Fairall, C.W., Bradley, E.F., Godfrey, J.S., Wick, G.A., Edson, J.B., Young, G.S., 1996b. Cool-skin and warm-layer effects on sea surface temperature. Journal of Geophysical Research 101, 1295–1308.

Fox, D.N., Teague, W.J., Barron, C.N., 2001. The Modular Ocean Data Assimilation System (MODAS). Journal of Atmospheric and Oceanic Technology 19, 240–252.

Fox, D.N., Barron, C.N., Carnes, M.R., Booda, M., Peggion, G., Gurley, J.V., 2002. The Modular Ocean Data Assimilation System (MODAS). Oceanography 15 (1), 22–28.

Haidvogel, D.B., Arango, H.G., Hedstrom, K., Beckmann, A., Malanotte-Rizzoli, P., Shchepetkin, A.F., 2000. Model evaluation experiments in the north Atlantic basin: simulations in non-linear terrain following coordinates. Dynamics of Atmospheres and Oceans 32, 239–281.

Jackett, D.R., McDougall, T.J., 1995. Minimal adjustment of hydrostatic profiles to achieve static stability. Journal of Atmospheric and Oceanic Technology 12, 381–389.

Ly L. N., Aikman III, F., Stumpf, R., Gross, T., 2004. Preliminary modeling of cross-shelf transport in support of monitoring and forecasting of harmful algal blooms along the west Florida coast. In: Proceedings Harmful Algae 2002, Xth HAB International Conference, St. Petersburg Beach, FL, USA, October 21–25, 2002, pp. 534–536.

Li, Z., Weisberg, R.H., 1999. West Florida shelf response to upwelling favorable wind forcing: kinematics. Journal of Geophysical Research 104, 13507–13527.

Liu, W.T., Katsaros, K.B., Businger, J.A., 1979. Bulk parameterization of the air-sea exchange of heat and water vapor including the molecular constraints at the interface. Journal of the Atmospheric Sciences 36, 1722–1735.

Lutjeharms, J.R.E., Penven, P., Roy, C., 2003. Modelling the shear edge eddies of the southern Agulhas current. Continental Shelf Research 23, 1099–1115.

MacCready, P., Geyer, W.R., 2001. Eastuarine salt flux through an isohaline surface. Journal of Geophysical Research 106, 11629–11637.

Marchesiello, P., McWilliams, J.C., Shchepetkin, A., 2001. Open boundary conditions for long-term integration of regional ocean models. Ocean Modelling 3, 1–20.

Marchesiello, P., McWilliams, J.C., Shchepetkin, A., 2003. Equilibrium structure and dynamics of the California current system. Journal of Physical Oceanography 33, 753–783.

Mellor, G.L., Yamada, T., 1982. Development of a turbulence closure model for geophysical fluid problems. Reviews of Geophysics and Space Physics 20, 851–875.

Modular Ocean Data Assimilation System (MODAS), 2005. http://www7320.nrlssc.navy.mil/modas/.

National Oceanic and Atmospheric Administration (NOAA)/National Geophysical Data Center (NGDC), 2004. http://www.ngdc.noaa.gov/.

Parkinson, C.L., Washington, W.M., 1979. A large-scale numerical model of sea ice. Journal of Geophysical Research 84 (C1), 311–337.

Peliz, A., Dubert, A.J., Haidvogel, D.B., 2003. Subinertial response of a density-driven eastern boundary poleward current to wind forcing. Journal of Physical Oceanography 33, 1633–1650.

Regional Ocean Modeling System (ROMS), 2005. http://www.imcs.rutgers.edu/po/index.php?models=roms.

Shchepetkin, A.F., McWilliams, J.C., 1998. Quasi-monotone advection schemes based on explicit locally adaptive dissipation. Monthly Weather Review 126, 1541–1580.

Shchepetkin, A.F., McWilliams, J.C., 2004. The Regional Oceanic Modeling System: a split-explicit, free-surface, topography-following-coordinate ocean model. Ocean Modelling 9 (4), 347–404.

Song, Y.T., Haidvogel, D.B., 1994. A semi-implicit ocean circulation model using a generalized topography following coordinate system. Journal of Computational Physics 115, 228–244.

Steidinger, K.A., Joyce, E.A., 1973. Florida Red Tides. State of Florida Department of Natural Resources Educational Series 17, 1–26.

Stumpf, R.P., Ransibrahmanakul, V., Steidinger, K.A., Tester, P.A., 1998. Observations of sea surface temperature and winds associated with Florida, USA, red tides (*Gymnodinium breve* blooms). In: Reguera, B., Blanco, J., Fernandez, M., et al. (Eds.), Harmful Algae, Proceedings of the VIII International Conference on Harmful Algae. Xunta de Galacia and IOC of UNESCO, Paris, France, pp. 145–148.

Stumpf, R.P., Culver, M.E., Tester, P.A., Tomlinson, M., Kirkpatrick, G.J., Pederson, B.A., Truby, E., Ransibrahmanakul, V., Soracco, M., 2003. Monitoring *Karenia brevis* blooms in the Gulf of Mexico using satellite ocean color imagery and other data. Harmful Algae 2, 147–160.

Tomlinson, M.C., Stumpf, R.P., Ransibrahmanakul, V., Truby, E.W., Kirkpatrick, G.J., Pederson, B.A., Vargo, G.A., Heil, C.A., 2004. Evaluation of the use of SeaWiFS imagery for detecting Karenia brevis harmful algal blooms in the eastern Gulf of Mexico. Remote Sensing of Environment 91, 293–303.

Walsh, J.J., Weisberg, R.H., Dieterle, D.A., He, R., Darrow, B.P., Jolliff, J.K., Lester, K.M., Vargo, G.A., Kirkpatrick, G.J., Fanning, K.A., Sutton, T.T., Jochens, A.E., Biggs, D.C., Nababan, B., Hu, C., Muller-Karger, F.E., 2003. Phytoplankton response to intrusions of slope water on the West Florida Shelf: models and observations. Journal of Geophysical Research 108, 3190–3212.

Warner, J.C., Sherwood, C.R., Arango, H.G., Signell, R.P., 2005. Performance of four turbulence closure methods implemented using a generic length scale method. Ocean Modelling 8, 81–113.